COMPARATIVE STUDY ON TiO_2 NANOPARTICLES OBTAINED BY PRECIPITATION AND SOL-GEL

Andrada-Elena ALECU[1], Stefania-Andreea GIRJOABA[2], Monica-Maria ENCULESCU[3], Cristina BUSUIOC[4]

The purpose of the work is the synthesis and characterization of TiO_2 nanoparticles. These were obtained by two different methods, precipitation and sol-gel, starting from titanium(IV) isopropoxide and calcining at 500 °C for 2 h. The compositional, structural, morphological and optical properties of the resulting powders were investigated by energy dispersive X-ray spectroscopy, Fourier transform infrared spectroscopy, X-ray diffraction, Raman spectroscopy, scanning electron microscopy, reflectance spectroscopy and photoluminescence spectroscopy. The thermally treated samples contain TiO_2 as single phase with tetragonal structure, known as anatase. SEM analysis showed quasi-spherical particles with a diameter of few nanometres for the calcined samples, while the optical studies revealed band gap values of 3.04 and 3.17 eV, as a function of the preparation route.

Keywords: TiO_2, nanoparticles, precipitation, sol-gel, band gap.

1. Introduction

Over time, it has been demonstrated that titanium dioxide (TiO_2) can be used in a wide variety of fields, such as painting industry [1], pharmaceutical industry [2], cosmetic industry [3], food industry [4], medicine [5]. In the last few years, researchers' attention has turned to materials with interesting properties and came up with new approaches for widespread development, like TiO_2; it is well-known as a semiconductor [6] that has optical [7], electrical [8] and catalytic properties [9]. Thus, more studies show the applicability and properties of TiO_2 for different applications, such as drug delivery and therapy [5, 10], antibacterial agents [11, 12] environmental applications [13], cosmetic sunscreens [3, 14], sensors [15, 16].

There are several routes for preparing TiO_2: hydrothermal [17, 18], sol-gel [19, 20], precipitation [21, 22], electrochemical [3, 23]. Among these, the most used approaches are precipitation and sol-gel, because of their simplicity and cost

[1] PhD Student, Department of Science and Engineering of Oxide Materials and Nanomaterials, University POLITEHNICA of Bucharest, Romania, e-mail: andrada_elena.alecu@upb.ro

[2] Student, Department of Bioengineering and Biotechnology, University POLITEHNICA of Bucharest, Romania, e-mail: stefania.girjoaba@stud.fim.upb.ro

[3] Scientific Researcher I, Laboratory of Multifunctional Materials and Structures, National Institute of Materials Physics, Romania, e-mail: mdatcu@infim.ro

[4] Associate Professor, Department of Science and Engineering of Oxide Materials and Nanomaterials, University POLITEHNICA of Bucharest, Romania, e-mail: cristina.busuioc@upb.ro

effectiveness [19, 24]. The main advantages of the sol-gel method are purity, high homogeneity and stoichiometry control of the obtained material [25], and it also provides flexibility to achieve TiO_2 with different morphologies, like wires, tubes, films etc. [19, 26, 27]. Nevertheless, the common problem is that it may generate low-crystallinity or amorphous products [28]. By using the sol-gel route, the particle size is easy to control [23], while the precipitation approach faces difficulty in controlling the particle size [29]. However, the precipitation method for obtaining TiO_2 is recognised as a simple and a low cost one [30].

TiO_2 nanoparticles can have three crystalline phases: anatase, rutile and brookite [31-33], and they can be synthesized from materials like chlorides [34], sulphates [35] and alkoxides [36]. Still, titanium tetraisopropoxide ($[Ti(OCH(CH_3)_2),]_4$) is the most used reagent in the preparation of TiO_2 [19, 32].

Spoiala *et al.* [37] integrated TiO_2 nanoparticles prepared through the sol-gel method in adsorbent composite membranes based on chitosan for the removal of toxic pollutants; the oxide concentration was kept below 5 %, however good photocatalytic and antimicrobial activities were attained, confirming the potential of such materials in complex water purification processes (removal of heavy metal ions, antibiotics and microorganisms). Jinga *et al.* [38] loaded 5 % TiO_2 nanoparticles synthesized by the precipitation route on fibrous membranes of polycaprolactone, a biodegradable polymer frequently employed in tissue engineering; the biological evaluation performed on mesenchymal stem cells demonstrated that this composite represents a support accepted by the cell cultures, displaying significant cell proliferation. Moreover, glass-ceramic porous scaffolds with TiO_2 crystalline domains were fabricated using bacterial cellulose as template and thermally treating at temperatures above 1000 °C; their morphology was either as a fluffy mass composed of micrograins and nanorods or as a well-interconnected *3D* structure crossed by large pores, but all samples showed good biocompatibility in relation to the same cell cultures as previously mentioned [39]. As well, sol-gel approach was used for coating silica fume particles with TiO_2 nanoparticles, resulting in improved photocatalytic activity in the first hours; due to their good pozzolanic activity, the composites were employed for 3 % substitution of Portland cement for the preparation of self-cleaning mortars, which led to higher compressive strengths compared to the reference [40].

In this work, the precipitation and sol-gel methods were used for the synthesis of TiO_2 nanoparticles. The novelty resides in the comparative investigation of the dried intermediates and 500 °C calcinated powders in terms of thermal, compositional, structural, morphological and optical properties, with emphasis on the influence of the processing route on the final characteristics.

2. Experimental procedure

Two types of titanium dioxide (TiO_2) were prepared by two different methods. The precipitation route involves the formation of a poorly soluble compound called compound, occurred in a liquid medium. It has the advantages of low manufacturing costs and lack of organic solvents. The sol-gel synthesis is an approach that resides in the hydrolysis of the precursors to form a colloidal solution (sol), which is followed by the polycondensation of –Ti–OH groups and then the formation of a network based on –Ti–O–Ti– bonds. As the network connectivity increases, so does the viscosity, thus forming the gel; it is then subjected to operations like drying and calcination or sintering. The main advantages are high purity and homogeneity, low processing temperatures and reduced particle size.

The samples were processed as described below.

1. For the precipitation, 40 mL of titanium(IV) isopropoxide ($Ti(O\text{-}i\text{-}Pr)_4$ = $Ti[OCH(CH_3)_2]_4$, M_W = 284.22 g/mol, p = 97 %, ρ = 0.96 g/mL) and 120 mL of isopropyl alcohol (i-PrOH = $(CH_3)_2CHOH$, M_W = 60.10 g/mol, $p \geq 98$ %) were mixed and 5 mL of distilled water were added, obtaining a white precipitate (pH = 7), which was filtered, washed and dried at 80 °C for 24 h.

2. For the sol-gel, the same quantities of titanium(IV) isopropoxide and isopropyl alcohol were mixed and nitric acid was added to reach a pH of 2.5. Approximately 2 min after the addition of 5 mL of distilled water, a gelation process occurred, the gel being dried in similar conditions as previously mentioned.

The thermal analysis was recorded from room temperature to 1000 °C, in air, on a Shimadzu DTG-60 equipment. The chemical bonds were studied by Fourier transform infrared (FTIR) spectroscopy, with a Thermo Scientific Nicolet iS50 spectrophotometer, in the attenuated total reflection (ATR) mode, the wavenumber ranging between 400 and 4000 cm^{-1}. The phase composition and crystal structure were revealed by X-ray diffraction (XRD), with a Shimadzu XRD 6000 diffractometer, using Ni-filtered Cu Kα radiation (λ = 1.54 Å), 2θ ranging between 10 and 60 °. The morphology was visualised by scanning electron microscopy (SEM), with a Quanta Inspect F microscope equipped with an energy-dispersive X-ray spectroscopy (EDX) probe for evaluating the elemental composition. The reflectance spectra were recorded with a Perkin Elmer Lambda 45 UV-Vis spectrophotometer equipped with an integrating sphere, while the photoluminescence spectra with a FL 920 Edinburgh Instruments spectrophotometer equipped with a Xe900 lamp.

3. Results and discussion

Fig. 1 displays the thermal analyses of the dried precipitate and gel. In the case of the precipitate, there are only two stages of weight loss on the DTG curve, the first being more intense than the second: around 23 % mass loss between 20 and 180 °C, as against around 3 % mass loss between 180 and 250 °C. These are generated by processes that take place simultaneously, starting with the evaporation of residual water and ending up with the decomposition of hydroxides / oxyhydroxides or the combustion of the organic part found in the system. Thus, endothermic and exothermic processes are overlapped in the DTA curve.

In the case of the gel, there are three stages of weight loss on the DTG curve in the temperature range 0-500 °C, after this threshold the loss being insignificant. The first one takes place in the range 20-190 °C, is around 15 % and corresponds to the elimination of the physically bound water (endothermic process). The second one takes place in the range 190-300 °C, being around 6 %, while the third one takes place in the range 300-500 °C, being around 3 %; these are associated with endothermic and exothermic processes, such as removal of the chemically bound water, burning of the organic part and other decomposition reactions.

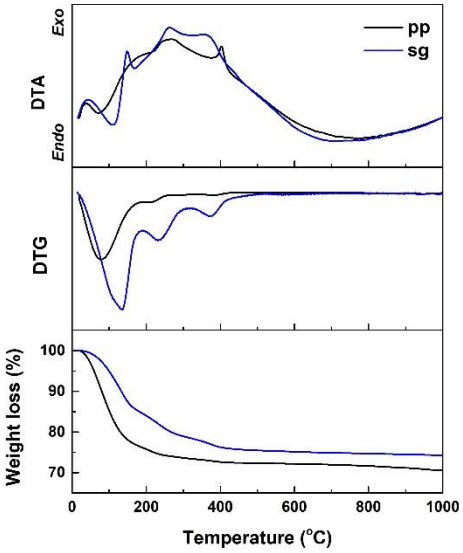

Fig. 1. Thermal analyses of the dried precipitate and gel.

The EDX spectra shown in Fig. 2a indicate the presence of Ti and O for both methods. The precipitate and gel also contain C, that disappears with the elimination of the reaction residues. Fig. 2b presents the FTIR spectra for the same samples, in which a reduced number of vibrational bands are available; at low

wavenumbers, Ti–O bonds are visible, while the uncalcined materials exhibit a large vibrational band at high wavenumbers, typical of OH groups.

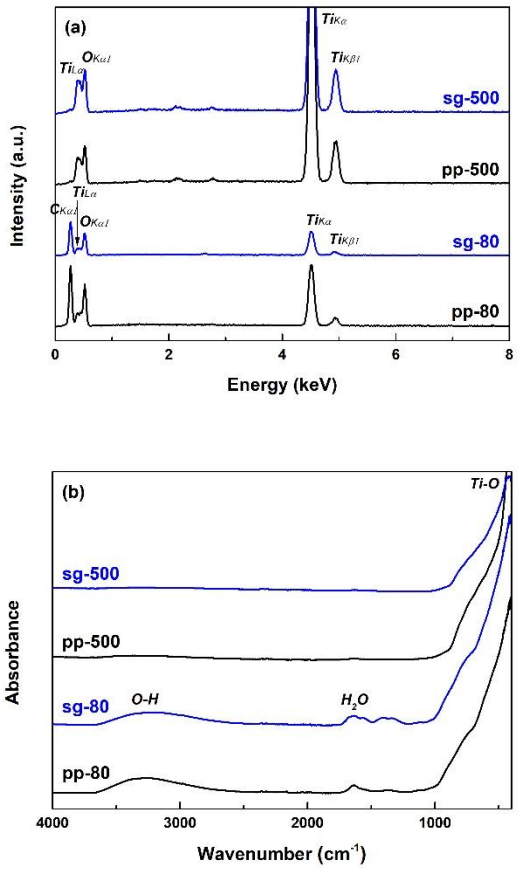

Fig. 2. (a) EDX and (b) FTIR spectra of the dried precipitate and gel, as well as powders calcined at 500 °C.

In terms of structure, the XRD patterns from Fig. 3a led to the identification of TiO_2 polycrystalline compound with tetragonal structure, known as anatase, based on the sheet ICCD 00-084-1286 from the database and the diffraction peaks located at 2θ angle of 25, 38, 48, 54, 56, 63 and 69 °. The two small peaks present in the upper XRD pattern and indicated by the star were also attributed to TiO_2 with tetragonal structure, but with different cell parameters, known as rutile (ICCD 00-084-1284). It can also be observed that an incipient crystallization is associated with the gel, whereas the precipitate is completely amorphous.

The long-range ordering was also investigated through Raman spectroscopy, the corresponding spectra being centralized in Fig. 3b. The transition from precipitate and gel to calcined powders is marked by the emergence of

vibrational bands with maxima at 140, 393, 512 and 637 cm^{-1}. The anatase-type tetragonal structure is demonstrated by these active Raman modes, representing a structural fingerprint easily identified and compatible with the data provided by the X-ray diffraction.

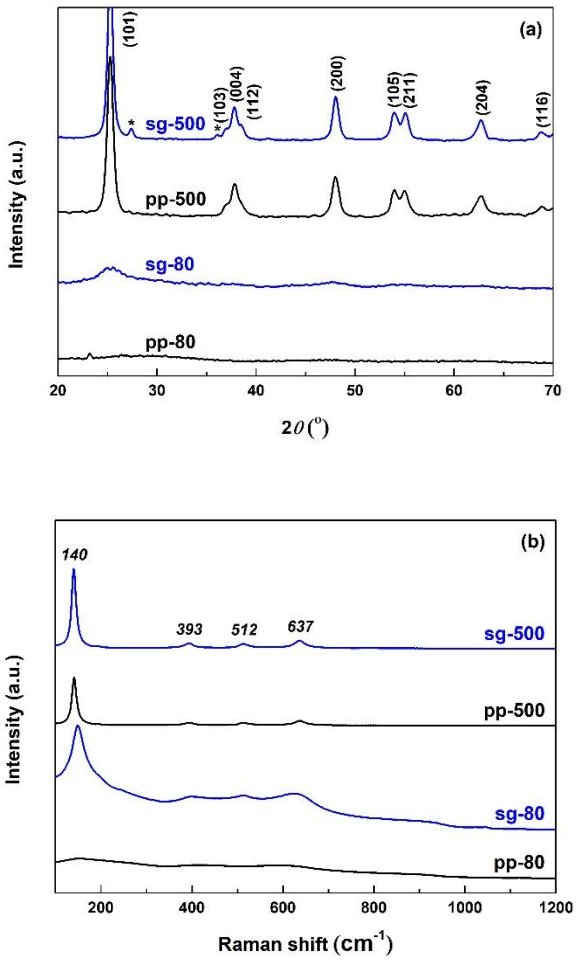

Fig. 3. (a) XRD patterns and (b) Raman spectra of the dried precipitate and gel, as well as powders calcined at 500 °C.

Fig. 4 presents the morphological features of the uncalcined and calcined samples. The dried precipitate is composed of micrometric entities that evolve towards a fine powder with fluffy aggregates and quasi-spherical particles of several nanometres' diameter (500 °C). The dried gel has a more inhomogeneous aspect, but also micrometric in size and with a discontinuous deposition on the surface; after calcination at 500 °C, the powder becomes coarser and more rugged at the level of the agglomerates, but nanometric at the level of individual particles.

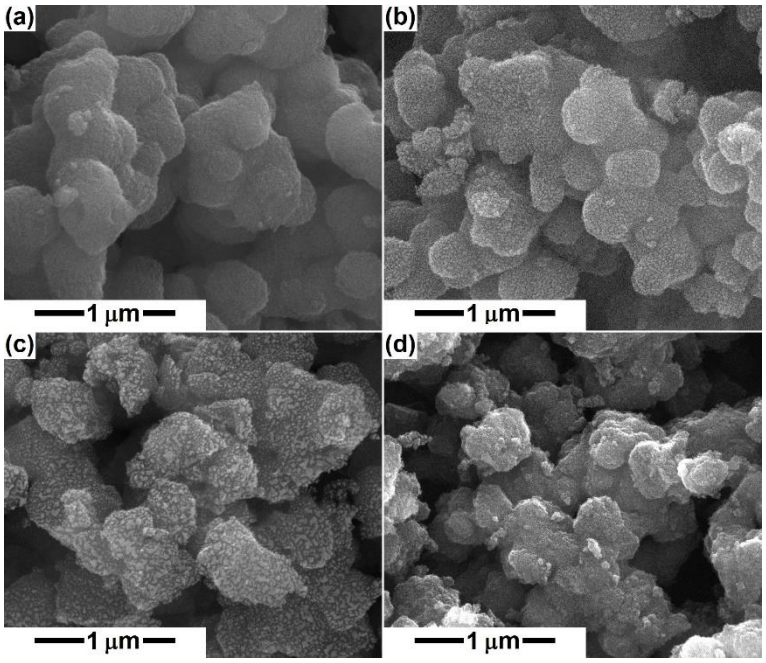

Fig. 4. SEM images of: (a) dried precipitate, (b) precipitate calcined at 500 °C, (c) dried gel and (d) gel calcined at 500 °C.

The optical properties of TiO_2 nanopowders calcined at 500 °C were also investigated, Fig. 5a showing the associated reflection spectra. The band-to-band transition in the semiconductor is highlighted by the pronounced decrease in reflectance below 450 nm. To estimate the band gap values, Kubelka-Munk functions (*F(R)*) were calculated and $[F(R)\cdot E]^{1/2}$ functions were plotted versus photon energy (*E*) (Fig. 5b). Kubelka-Munk function is expressed as $F(R)=(1-R)^2/(2\cdot R)$, where *R* is the observed diffuse reflectance. The resulting band gap values are 3.17 eV for the precipitation method and 3.04 eV for the sol-gel route, similar or slightly lower compared to what other researchers obtained [9, 21, 41, 42]. A slight decrease in the band gap is observed with the transition from the precipitation approach to the sol-gel one, but this cannot be solely attributed to the phase composition; the particle size and defects concentration in the crystalline network are also important parameters. The scientific literature mentions a larger bandgap energy for anatase compared to rutile (3.2 eV *vs.* 3.0 eV), this deriving from the electronic configuration, atomic distance and mass density.

Photoluminescence (PL) emissions result from the recombination of free charge carriers in a semiconductor, which means that a lower PL intensity indicates lower charge recombination. In general, PL spectra are due to self-trapped excitons, oxygen vacancies and surface states [43].

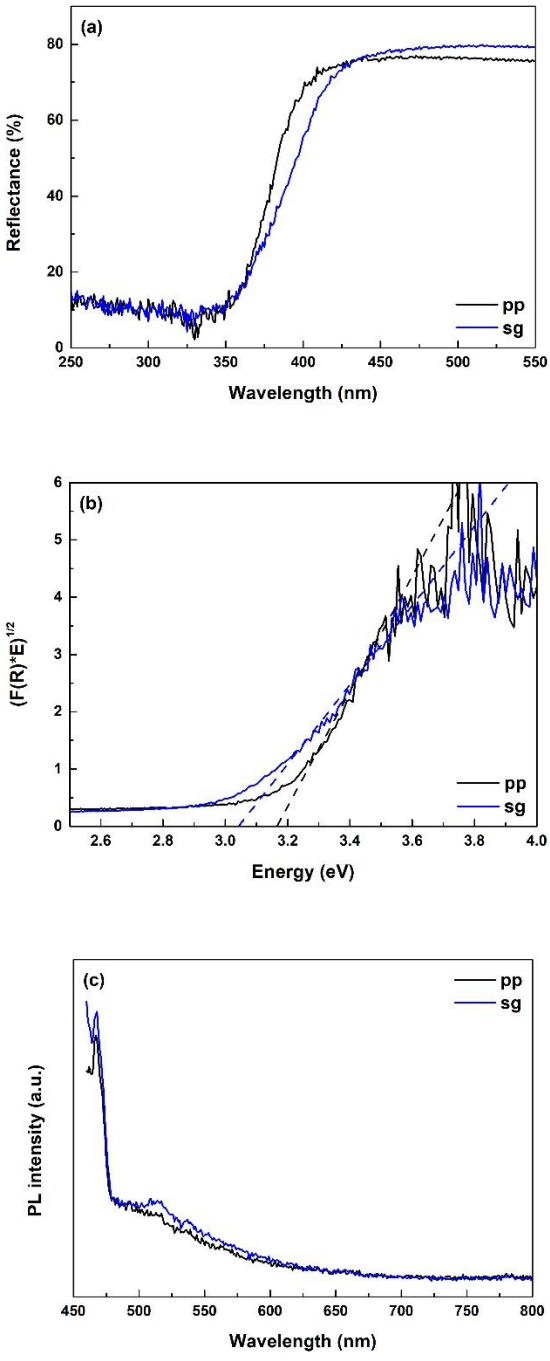

Fig. 5. (a) Reflectance spectra, (b) Kubelka-Munk functions and (c) PL spectra of TiO_2 powders.

The PL spectra of the final samples were recorded, with excitation at 440 nm. In Fig. 5c, the sharp and intense emission band centred at around 470 nm is assigned to the self-trapped excitons, whereas the broad and small one with maximum at around 510 nm is due to oxygen vacancies [42]. The slight increase in intensity from the precipitation route to the sol-gel one indicates that the recombination process of electrons and holes is favoured, fact that is consistent with the previous statements regarding the band gap energy. Anyway, no shift or important intensity increase/decrease of the emission bands is visible, which suggest that the low content of rutile in the sample processed by the sol-gel route does not significantly influence the optical properties and subsequent catalytic performances, that are known to be better in the case of anatase; unfortunately, no consensus exists upon the reasons for this behaviour.

4. Conclusions

TiO_2 nanopowders with anatase-like tetragonal crystalline structure were successfully synthesized by the precipitation and sol-gel methods, with calcination at 500 °C for 2 h. The thermal analysis evidenced a more complex transition, with several weight loss stages and thermal processes in the case of the gel than in the case of the precipitate. As well, an incipient crystallization was revealed only for the gel, which also displayed a small amount of secondary phase with rutile-like tetragonal crystalline structure after calcination, while the calcined precipitate was a single-phase powder. The resulting quasi-spherical particles exhibit diameters below 10 nm, slightly smaller in the case of the sol-gel route. Band gap values of 3.17 and 3.04 eV were determined for the precipitation and sol-gel approaches, respectively, aspect correlated with slightly more intense emissions under 440 nm excitation for the calcined gel. Such nanometric semiconducting powders prepared by simple methods can be used for applications in the field of electronics, catalysis, sensors, antibacterial agents etc.

Acknowledgement

This work was supported by the grant POCU/993/6/13-153178, co-financed by the European Social Fund within the Sectorial Operational Program Human Capital 2014-2020.

R E F E R E N C E S

[1] *T. Rezende, J. Silvestre, P. Mendonca, J. Moniz, A. Serra, J. Coelho*, Efficient Dispersion of TiO_2 in Water-Based Paint Formulation Using Well-Defined Poly[oligo(ethylene oxide) methyl ether acrylate] Synthesized by ICAR ATRP, Progress in Organic Coatings 165 (2022) 106734.

[2] *R. Aswini, S. Murugesan, K. Kannan*, Bio-engineered TiO_2 Nanoparticles Using *Ledebouria Revoluta* Extract: Larvicidal, Histopathological, Antibacterial and Anticancer Activity, International Journal of Environmental Analytical Chemistry 101 [15] 2926−2936 (2021).
[3] *B. Dreno, A. Alexis, B. Chuberre, M. Marinovich*, Safety of Titanium Dioxide Nanoparticles in Cosmetics, Journal of the European Academy of Dermatology and Venereology 33 [S7] 34−46 (2019).
[4] *A. Berardinelli, F. Parisi*, TiO_2 in the Food Industry and Cosmetics, in Titanium Dioxide (TiO_2) and Its Applications (2021) 353−371.
[5] *S. Cesmeli, C. Biray Avci*, Application of Titanium Dioxide (TiO_2) Nanoparticles in Cancer Therapies, Journal of Drug Targeting 27 [7] 762−766 (2019).
[6] *G. Yang, Z. Jiang, H. Shi, M.O. Jones, T. Xiao, P.P. Edwards, Z. Yan*, Study on the Photocatalysis of F-S Co-doped TiO_2 Prepared Using Solvothermal Method, Applied Catalysis B: Environmental 96 (2010) 458−465.
[7] *A. Ali, S. Zareen, M. Irfan*, The Effect of Annealing Temperatures on Phase and Optical Properties of TiO_2 Nanoparticles for Solar Cell Applications, European Scientific Journal 2 (2014) 447−450.
[8] *A. Arunachalam, S. Dhanapandian, C. Manoharan*, Effect of Sn Doping on the Structural, Optical and Electrical Properties of TiO_2 Films Prepared by Spray Pyrolysis, Physica E: Low-dimensional Systems and Nanostructures 76 (2015) 35−46.
[9] *M.S. Hassan, A.I. Ahmed, M.A. Mannaa*, Structural, Photocatalytic, Biological and Catalytic Properties of SnO_2/TiO_2 Nanoparticles, Ceramics International 44 [6] 6201−6211 (2018).
[10] *T. Wang, H. Jiang, L. Wan, Q. Zhao, T. Jiang, B. Wang, S. Wang*, Potential Application of Functional Porous TiO_2 Nanoparticles in Light-Controlled Drug Release and Targeted Drug Delivery, Acta Biomaterialia 13 (2015) 354−363.
[11] *P. Anandgaonker, G. Kulkarni, S. Gaikwad, A. Rajbhoj*, Synthesis of TiO_2 Nanoparticles by Electrochemical Method and Their Antibacterial Application, Arabian Journal of Chemistry 12 [8] 1815−1822 (2019).
[12] *Y. Yuan, J. Ding, J. Xu, J. Deng, J. Guo*, TiO_2 Nanoparticles Co-doped with Silver and Nitrogen for Antibacterial Application, Journal of Nanoscience and Nanotechnology 10[8] 4868−4874 (2010).
[13] *A. Haider, R. Al-Anbari, G. Kadhim, C. Salame*, Exploring Potential Environmental Applications of TiO_2 Nanoparticles, Energy Procedia 119 (2017) 332−345.
[14] *P.J. Lu, S.C. Huang, Y.P. Chen, L.C. Chiueh, D.Y.C. Shih*, Analysis of Titanium Dioxide and Zinc Oxide Nanoparticles in Cosmetics, Journal of Food and Drug Analysis 23 [3] 587−594 (2015).
[15] *D. Zhao, X. Zhang, W. Wang, L. Sui, C. Guo, Y. Xu, X. Cheng, S. Gao, L. Huo*, Ultra-small TiO_2 Nanocubes with Highly Active (001) Facet for Acetone fast Detection and Diagnosis of Diabetes, SSRN Electronic Journal (2022) DOI:10.2139/ssrn.4180270.
[16] *K. Wu, W. Zhang, Z. Zheng, M. Debliqui, C. Zhang*, Room-temperature Gas Sensors Based on Titanium Dioxide Quantum Dots for Highly Sensitive and Selective H_2S Detection, Applied Surface Science 585 (2022) 152744.
[17] *J.B. Shi, G.Q. Chen, G.M. Zeng, A. Chen, K. He, Z.Z. Huang, L. Hu, J.W. Zeng, J. Wu, W.W. Liu*, Hydrothermal Synthesis of Graphene Wrapped Fe-doped TiO_2 Nanospheres with High Photocatalysis Performance, Ceramics International 44 [7] 7473−7480 (2018).
[18] *T. Oekermann, D.S. Zhang, T. Yoshida, H. Minoura*, Electron Transport and Back Reaction in Nanocrystalline TiO_2 Films Prepared by Hydrothermal Crystallization, Journal of Physical Chemistry B 108 (2004) 72227−72235.
[19] *A. Sharma, R.K. Karn, S.K. Pandiyan*, Synthesis of TiO_2 Nanoparticles by Sol-gel Method and Their Characterization 1 [9] 1−5 (2014).

[20] *V.T. Lukong, K.O. Ukoba, T.C. Jen*, Heat-assisted Sol-gel Synthesis of TiO_2 Nanoparticles Structural, Morphological and Optical Analysis for Self-cleaning Application 34 [1] 101746 (2022).

[21] *T. Kalaivani, P. Anilkumar*, Role of Temperature on the Phase Modification of TiO_2 Nanoparticles Synthesized by the Precipitation Method, Silicon 10 [4] 1679−1686 (2018).

[22] *Z. Wang, S. Liu, X. Cao, S. Wu, C. Liu, G. Li, W. Jiang, H. Wang, N. Wang, W. Ding*, Preparation and Characterization of TiO_2 Nanoparticles by Two Different Precipitation Methods, Ceramics International 46 [10] 15333−15341 (2020).

[23] *P. Nyamukamba, O. Okoh, H. Mungondori, R. Taziwa S. Zinya*, Synthetic Methods for Titanium Dioxide Nanoparticles: A Review, in Titanium Dioxide - Material for a Sustainable Environment 8 (2018) 151−175.

[24] *S.M. Gupta, M. Tripathi*, A Review on the Synthesis of TiO_2 Nanoparticles by Solution Route, Central European Journal of Chemistry 10 [2] 279−294 (2012).

[25] *N. Wetchakun, S. Phanichphant*, Effect of Temperature on the Degree of Anatase-rutile Transformation in Titanium Dioxide Nanoparticles Synthesized by the Modified Sol-gel Method, Current Applied Physics 8 (2008) 343−346.

[26] *L. Bazli, M. Siavashi, A. Shiravi*, A Review of Carbon Nanotube/TiO_2 Composite Prepared via Sol-gel Method, Journal of Composites and Compounds 1 [1] 1−9 (2019).

[27] *M.J. Alam, D.C. Cameron*, Preparation and Characterization of TiO_2 Thin Films by Sol-Gel Method, Journal of Sol-Gel Science and Technology 25 (2002) 137−145.

[28] *E. Cerro-Prada, S. Garcia-Salgado, M.A. Quijano, F. Varela*, Controlled Synthesis and Microstructural Properties of Sol-Gel TiO_2 Nanoparticles for Photocatalytic Cement Composites, Nanomaterials 9 [1] 26 (2018).

[29] *M.S. Waghmode, A.B. Gunjal, J.A. Mulla, N.N. Patil, N.N. Nawani*, Studies on the Titanium Dioxide Nanoparticles: Biosynthesis, Applications and Remediation. SN Applied Sciencies 1 (2019) 310.

[30] *S. Sugapriya, R. Sriram, S. Lakshmi*, Effect of Annealing on TiO_2 Nanoparticles, Optik 124 (2013) 4971−4975.

[31] *V. Mansfeldova, M. Zlamalova, H. Tarabkova, P. Janda, M. Vorokhta, L. Piliai, L. Kavan*, Work Function of TiO_2 (Anatase, Rutile, and Brookite) Single Crystals: Effects of the Environment, Journal of Physical Chemistry C 125 [3] 1902−1912 (2021).

[32] *Zerjav, K. Zizek, J. Zavasnik, A. Pintar*, Brookite vs. Rutile vs. Anatase: What's Behind Their Various Photocatalytic Activities? Journal of Environmental Chemical Engineering 10 [3] 107722 (2022).

[33] *S.A. Hamdan, I.M. Ibrahim, I.M. Ali*, Comparison of Anatase and Rutile TiO_2 Nanostructure for Gas Sensing Application, Digest Journal of Nanomaterials and Biostructures 15 [4] 1001−1008 (2020).

[34] *R. Alexandrescu, I. Morjan, M. Scarisoreanu, E. Popovici, I. Soare, L. Gavrila-Florescu, I. Voicu, I. Sandu, F. Dumitrache, G. Prodan, E. Vasile, E. Figgemeierl*, Structural Investigations on TiO_2 and Fe-doped TiO_2 Nanoparticles Synthesized by Laser Pyrolysis, Thin Solid Films 515 (2007) 8438−8445.

[35] *A. Zhang, N. Huang, Y. He, P. Zhao, J. Feng*, Sulfate Radicals' Generation and Refractory Pollutants Removal on Defective Facet-tailored TiO_2 with Reduced Matrix Effects, Chemical Engineering Journal 358 (2019) 243−252.

[36] *G. Oskam, A. Nellore, R.L. Penn, P.C. Searson*, The Growth Kinetics of TiO_2 Nanoparticles from Titanium (IV) Alkoxide at High Water/titanium Ratio, Journal of Physical Chemistry B 1078 (2003) 1734−1738.

[37] *A. Spoiala, C.I. Ilie, G. Dolete, A.M. Croitoru, V.A. Surdu, R.D. Trusca, L. Motelica, O.C. Oprea, D. Ficai, A. Ficai, E. Andronescu, L.M. Ditu*, Preparation and Characterization of

Chitosan/TiO_2 Composite Membranes as Adsorbent Materials for Water Purification, Membranes 12 (2022) 804.

[38] *S.I. Jinga, A.I. Zamfirescu, G. Voicu, M. Enculescu, A. Evanghelidis, C. Busuioc*, PCL-ZnO/TiO_2/HAp Electrospun Composite Fibres with Applications in Tissue Engineering, Polymers 11 (2019) 1793.

[39] *S.I. Jinga, A.D. Draghici, A. Mocanu, A.I. Nicoara, F. Iordache, C. Busuioc*, Bacterial Cellulose-Assisted Synthesis of Glass-Ceramic Scaffolds with TiO_2 Crystalline Domains, International Journal of Applied Ceramic Technology 17 (2020) 2017–20124.

[40] *A.V. Zanfir, G. Voicu, A. Badanoiu, D. Gogan, O. Oprea, E. Vasile*, Synthesis and Characterization of Titania-Silica Fume Composites and Their Influence on the Strength of Self-Cleaning Mortar, Composites B 140 (2018) 157–163.

[41] *S. Prasad, S.S. Kumar, V.P.M. Shajudheen*, Synthesis, Characterization and Study of Photocatalytic Activity of TiO_2 Nanoparticles, Materials Today: Proceedings 33 [5] 2286−2288 (2020).

[42] *F.Z. Haque, R. Nandanwar, P. Singh*, Evaluating Photodegradation Properties of Anatase and Rutile TiO_2 Nanoparticles for Organic Compounds, Optik 128 (2017) 191−200.

[43] *D.K. Pallotti, L. Passoni, P. Maddalena, F. Di Fonzo, S. Lettieri*, Photoluminescence Mechanisms in Anatase and Rutile TiO_2, The Journal of Physical Chemistry C 121 (2017) 9011−9021.